Science of the Total Environment 919 (2024) 170726

Contents lists available at ScienceDirect

Science of the Total Environment

journal homepage: www.elsevier.com/locate/scitotenv

Drought alters aboveground biomass production efficiency: Insights from two European beech forests

Jingshu Wei [a,b,c,*], Georg von Arx [b,d], Zexin Fan [c], Andreas Ibrom [e], Martina Mund [f], Alexander Knohl [g], Richard L. Peters [h], Flurin Babst [a,i]

[a] School of Natural Resources and the Environment, University of Arizona, 1064 E Lowell Street, Tucson, AZ 85721, USA
[b] Swiss Federal Institute for Forest Snow and Landscape Research WSL, Zuercherstrasse 111, CH-8903 Birmensdorf, Switzerland
[c] CAS Key Laboratory of Tropical Forest Ecology, Xishuangbanna Tropical Botanical Garden, Chinese Academy of Sciences, Menglun Town, Mengla County, Yunnan Province 666303, China
[d] Oeschger Centre for Climate Change Research, University of Bern, Hochschulstrasse 4, CH-3012 Bern, Switzerland
[e] Biosystems Division, Risø National Laboratory for Sustainable Energy, Technical University of Denmark, Denmark
[f] Forestry Research and Competence Centre Gotha, Jägerstraße1, D-99867 Gotha, Germany,
[g] Bioclimatology, University of Göttingen, Büsgenweg 2, D-37077 Göttingen, Germany
[h] Environmental Sciences – Botany, University of Basel, Schönbeinstrasse 6, Basel CH-4056, Switzerland
[i] Laboratory of Tree-Ring Research, University of Arizona, 1215 E Lowell Street, Tucson, AZ 85721, USA

HIGHLIGHTS

- Carbon allocation to woody biomass in European beech is sink limited.
- Drought causes beech to de-prioritize wood formation in favor of other processes.
- Gross primary productivity recovers more rapidly from drought than tree growth.
- The timing of drought determines if growth is reduced in the current or next year.

GRAPHICAL ABSTRACT

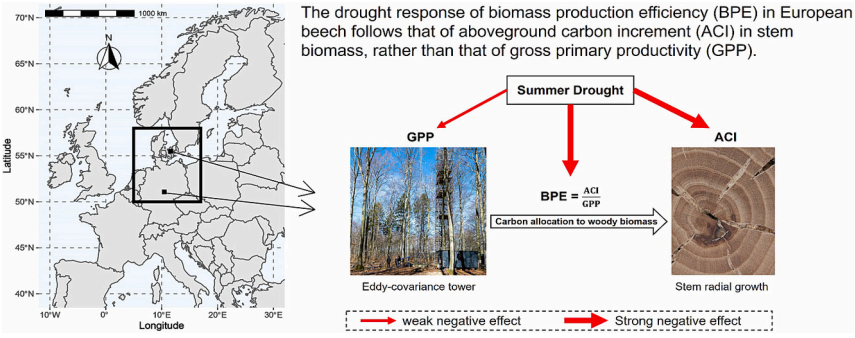

ARTICLE INFO

Editor: Manuel Esteban Lucas-Borja

Keywords:
Fagus sylvatica L
Carbon allocation
Tree growth
Gross primary productivity
Eddy covariance
Climate response
Drought extremes

ABSTRACT

The fraction of photosynthetically assimilated carbon that trees allocate to long-lasting woody biomass pools (biomass production efficiency – BPE), is a key metric of the forest carbon balance. Its apparent simplicity belies the complex interplay between underlying processes of photosynthesis, respiration, litter and fruit production, and tree growth that respond differently to climate variability. Whereas the magnitude of BPE has been routinely quantified in ecological studies, its temporal dynamics and responses to extreme events such as drought remain less well understood. Here, we combine long-term records of aboveground carbon increment (ACI) obtained from tree rings with stand-level gross primary productivity (GPP) from eddy covariance (EC) records to empirically quantify aboveground BPE (= ACI/GPP) and its interannual variability in two European beech forests (Hainich, DE-Hai, Germany; Sorø, DK-Sor, Denmark). We found significant negative correlations between BPE and a daily-

* Corresponding author at: School of Natural Resources and the Environment, University of Arizona, 1064 E Lowell Street, Tucson, AZ 85721, USA.
E-mail address: jwei@arizona.edu (J. Wei).

https://doi.org/10.1016/j.scitotenv.2024.170726
Received 5 September 2023; Received in revised form 3 February 2024; Accepted 3 February 2024
Available online 6 February 2024

resolved drought index at both sites, indicating that woody growth is de-prioritized under water limitation. During identified extreme years, early-season drought reduced same-year BPE by 29 % (Hainich, 2011), 31 % (Sorø, 2006), and 14 % (Sorø, 2013). By contrast, the 2003 late-summer drought resulted in a 17 % reduction of post-drought year BPE at Hainich. Across the entire EC period, the daily-to-seasonal drought response of BPE resembled that of ACI, rather than that of GPP. This indicates that BPE follows sink dynamics more closely than source dynamics, which appear to be decoupled given the distinctive climate response patterns of GPP and ACI. Based on our observations, we caution against estimating the magnitude and variability of the carbon sink in European beech (and likely other temperate forests) based on carbon fluxes alone. We also encourage comparable studies at other long-term EC measurement sites from different ecosystems to further constrain the BPE response to rare climatic events.

1. Introduction

Carbon allocation to long-lasting woody biomass pools such as tree stems is an important process that co-determines the forest carbon sink dynamics. How many resources trees invest in woody growth is not only relevant from an ecological perspective, but also from a human perspective. The latter is with regard to nature-based climate solutions (Anderegg et al., 2022; Giebink et al., 2022; Hemes et al., 2021; Novick et al., 2022), timber production (Johnston and Radeloff, 2019), forest management (Calfapietra et al., 2015; Thürig and Kaufmann, 2010), or assessment of wildfire risk (Nolan et al., 2022). Two important processes that drive carbon allocation to tree stems are 1) carbon fixation through photosynthesis (gross primary productivity, GPP = carbon source for the tree and sink for the atmosphere) and 2) carbon sequestration through wood formation processes that drive the allocation of carbon to long-lasting structural biomass (herein quantified by the aboveground carbon increment, ACI = carbon sink). Other processes such as fine root, foliage, and fruit production also affect a tree's growth and carbon sink capacity but are associated with large uncertainties (Pugh et al., 2020; Yang et al., 2021) and not explicitly quantified in this study. The "biomass production efficiency" (BPE = ACI/GPP) of trees is thus defined as the fraction of GPP that is sequestered in structural woody biomass and is a key metric for the long-term forest carbon sink (Campioli et al., 2015; He et al., 2020; Vicca et al., 2012).

Environmental drivers of carbon source and sink dynamics in trees are varied, complex, and expected to shift under global change (Fatichi et al., 2014; Friend et al., 2019). For example, a recent meta-analysis of global flux-tower and tree-ring data has concluded that GPP and tree growth are largely decoupled and under different environmental constraints (Cabon et al., 2022) but without comparing the two processes quantitatively. GPP can respond to drought via stomatal limitation, which is both a reaction to soil water shortage and high atmospheric water demand. In addition, both GPP and CO_2 losses through autotrophic respiration (Ra) are temperature sensitive, but variation in Ra is caused by multiple pathways and processes in different tree organs, which are differently affected by environmental drivers and tree internal regulations compared to GPP. The remainder of the sequestered carbon, net primary productivity (NPP = GPP-Ra), is available to be allocated to different non-structural and structural sinks, including ACI (Fig. 1). The ACI is primarily achieved through the processes of wood formation, which are strongly influenced by turgor pressure and thus highly drought sensitive (Peters et al., 2020a; Peters et al., 2023). Given that GPP and ACI respond differently to climatic variability, we can expect BPE to shift during drought episodes and particularly during extreme events. This re-prioritization of resources has, however, rarely been quantified in empirical studies.

We have adopted BPE as a conceptually simple quantitative metric of carbon allocation to woody biomass that is, however, not straightforward to measure in-situ. The required measurements of both GPP and ACI can only be achieved at a relatively small number of ecological monitoring sites (<100 sites worldwide; Babst et al., 2021) where carbon fluxes have been continuously recorded using the eddy covariance (EC) method for the past one to three decades. Such long time series are key to assess BPE trajectories and its response to climatic variability and extremes. Combined tree-ring and biometric measurements from within the footprint area of a flux tower are thereby the preferred option to quantify stand-level ACI retrospectively, which requires a spatially representative sampling approach that differs from traditional dendrochronological data collection (Evans et al., 2022; Klesse et al., 2018; Nehrbass-Ahles et al., 2014). The number of existing studies that have quantified BPE this way has remained modest and these studies have drawn a varied picture of the magnitude, environmental constraints, and temporal variability of forest carbon allocation (e.g. Babst et al., 2014; Mund et al., 2020; Pappas et al., 2023; Pappas et al., 2020; Teets et al., 2018).

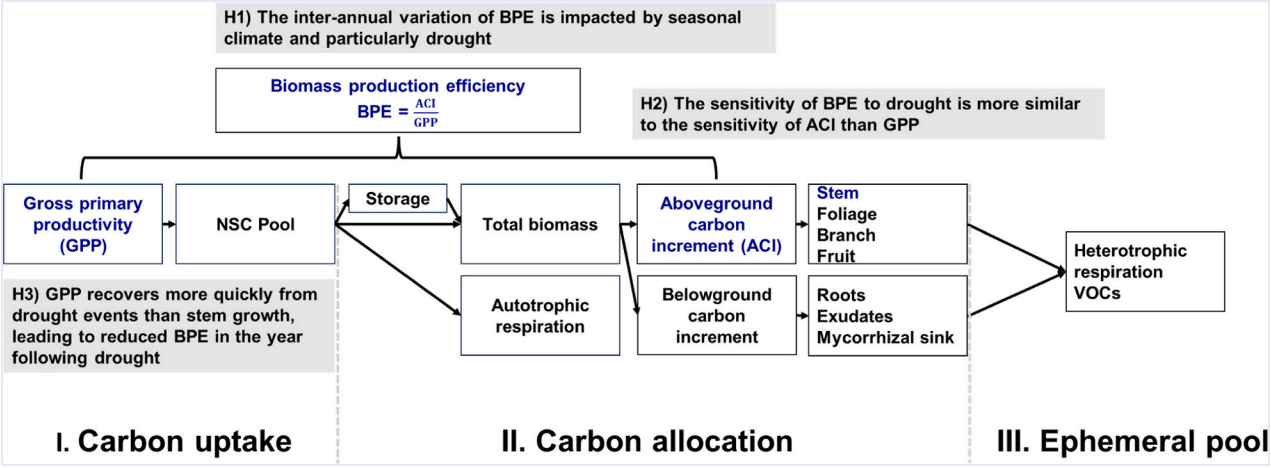

Fig. 1. Conceptual diagram illustrating the processes of carbon allocation along with three hypotheses investigated in our study. Note: Parameters in blue were utilized for analysis. Stem growth is represented by the tree-ring width index (TRI), NSC refers to non-structural carbohydrates, and VOCs refers to volatile organic compounds.

Environmental stressors, such as drought, can have pronounced impacts on a tree's physiology and in particular growth that can last for several years and alter carbon allocation within an ecosystem (Anderegg et al., 2015). Currently, however, there is a shortage of quantitative analyses regarding the variations of BPE under changing climatic conditions and over longer timescales. Therefore, it is crucial to understand if the BPE ratio depends more on GPP or ACI, and if it changes with reduced water availability. Clarifying these connections will improve our understanding of carbon allocation dynamics and help enhance land-surface models, which often predict vegetation carbon budgets solely based on GPP (Zuidema et al., 2018). Trees have the capacity to flexibly allocate the carbon obtained from GPP towards various sinks; this allocation can depend on factors such as climatic conditions, nutrient and light availability. In this respect, evidence is mounting that stem growth has a relatively low priority when environmental factors become limiting (Merganicova et al., 2019; Peters et al., 2020a; Sevanto and Dickman, 2015; Xia et al., 2017). Instead, carbon allocation is re-prioritized towards other sinks (Fig. 1, process II), including foliage (Kannenberg et al., 2019b), reproduction (Mund et al., 2020), roots (Miao et al., 2022), and non-structural carbohydrate storage (Carbone et al., 2013; Huang et al., 2021). Carbon that is allocated away from growth can also be released as volatile organic compounds (VOCs) for communication and defense purposes (Fig. 1, process III). As such, we anticipate that stem growth-related processes exhibit a higher sensitivity to drought compared to GPP (Kannenberg et al., 2019b; Peters et al., 2020b).

European beech (*Fagus sylvatica L.*) ranks among Europe's most abundant forest species (van der Werf et al., 2007) and contributes to a mean long-term carbon sink of ca. 75 g C m^{-2} yr^{-1} (Luyssaert et al., 2010). These beech forests have demonstrated a certain tolerance, plasticity, and resilience in their response to drought (Dyderski et al., 2018). However, the continuous rise in aridity, coupled with the occurrence of extreme droughts, poses a significant challenge to the productivity and survival of beech forests in their present state (Bosela et al., 2018). At sites with a pronounced drought limitation of beech forests, we expect that growth will be sink-limited and that the drought sensitivity of BPE would resemble that of ACI. If so, drought would reduce the capacity of beech trees to function as effective long-term carbon sinks. Testing this hypothesis is important because droughts are predicted to become more frequent and intense with climate change (Chiang et al., 2021). It is also challenging, because extreme events are rare by definition and existing flux-tower records are still relatively short. Despite these data constraints, we are now entering a time when BPE can be quantified over sufficiently long timescales to assess the impact of at least a limited number of drought events on stand-level carbon allocation (Kannenberg et al., 2022).

In this study, our objectives were as follows: 1) To quantify the annual variation of BPE empirically at two long-standing flux-tower sites in European beech stands, namely Hainich (DE-Hai, 2000–2018) and Sorø (DK-Sor, 1997–2017); 2) to compare the daily-to-seasonal climate sensitivities of BPE, GPP, and ACI; 3) to assess the impacts of drought extremes on these three metrics to identify priorities for carbon allocation under restrictive conditions. We tested the following guiding hypotheses: H1) The interannual variation of BPE is impacted by drought because GPP and ACI respond differently to water availability and demand (Cabon et al., 2022), H2) The climate sensitivity of BPE is more similar to that of ACI than that of GPP because drought induces turgor-limited growth (Peters et al. 2021), and H3) GPP recovers more quickly from drought events than stem growth (Peters et al., 2020a), leading to reduced BPE in the year following drought.

2. Materials and methods

2.1. Study sites

Our sampling sites are located at two well-studied and long-term ecological research stations in European beech forests with over two decades of eddy-covariance monitoring (see Table 1 and Fig. S1 for site locations). Both sites, Hainich (DE-Hai, Knohl et al., 2003), and Sorø (DK-Sor; see Peters et al., 2020a) are part of the FLUXNET network (see https://fluxnet.fluxdata.org), as well as the Integrated Carbon Observation System (ICOS; https://www.icos-cp.eu), and have adopted the respective measurement and data standards (Sabbatini et al., 2018). The long-term records with full-year data of carbon and water fluxes start in 2000 and 1997 for Hainich and Sorø, respectively, and continues presently.

Hainich (51°04′45″ N, 10°27′07″E, 430 m a.s.l) is located in the core zone of the Hainich National Park, Thuringia, Germany. The climate is suboceanic–submontane, with mean annual temperatures of 8.3 °C and mean precipitation of 732 mm. The soil is composed of an underlying Triassic limestone and covered with variable Pleistocene loess deposits. The tree species composition within our sampling plot and the entire flux-tower footprint is a mixture of the dominating European beech (*Fagus sylvatica L.*), with European ash (*Fraxinus excelsior L.*), sycamore maple (*Acer pseudoplatanus L.*), and a small fraction of additional deciduous species (Mund et al., 2020). The site has been unmanaged for roughly a century, so that it can be characterized as a near-naturally growing beech forest.

Sorø (55°29′13″ N, 11°38′45″E2, 40 m a.s.l) is located in the middle of the Lille Bøgeskov forest on the island of Zealand, about 80 km southwest of Copenhagen. The climate is temperate maritime, with mean annual temperatures of 8.5 °C and annual precipitation of 891 mm based

Table 1
Stand characteristics of the two European beech sampling sites. Mean values are given with +/− one standard deviation.

	Hainich (DE-Hai)	Sorø (DK-Sor)
Location	51°04′45″ N 10°27′07″ E	55°29′13″ N 11°38′45″ E
Elevation (m a.s.l.)	440	40
Management	Unmanaged	Thinning of 10 % per 10 years
Stand age range[a]	Uneven-aged stand, 47–234 yrs.	Mostly even-aged, 49–94 yrs
Annual precipitation sum (mm)[b]	732 ± 156	891 ± 299
Mean annual temperature (°C)[b]	8.3 ± 0.7	8.5 ± 0.6
Plot area (m^2)	2827	2460
Arithmetic mean tree height (m)	21.5 ± 11.4	26.0 ± 9.8
Arithmetic mean tree DBH (cm)	33.2 ± 27.1	39.4 ± 18.3
Number of sampled trees	89	54
Tree density (stems ha^{-1})	325	207
Tree-ring period	1785–2018	1924–2017
Analyzed eddy flux period	2000–2019	1997–2017
Substrate	Triassic limestone	Alfisols, Mollisols

[a] Stand age range is based on the tree-ring records within the stands.
[b] Annual mean temperature and precipitation sums were calculated from local meteorological data during the common period 2000–2017 between the two sites.

on the local meteorological record from 2000 to 2017. The soils are brown soils and classified as either Alfisols or Mollisols (depending on a base saturation of under or over 50 %) with a 10–40 cm deep organic layer (Pilegaard and Ibrom, 2020; Wu et al., 2013). The forest is mainly dominated by *Fagus sylvatica* L. with few scattered other tree species such as *Picea abies* and *Larix decidua*. The trees in the forest stand were planted around 1920 following a clearcut. Recently, a forest management regime with a thinning of 10 % of the basal area every 10 years has been implemented (Pilegaard and Ibrom, 2020). Further site details are provided in Table 1.

2.2. Field sample collection

In 2018 and 2019, we established sampling plots within the primary footprint areas of the flux towers, known from local footprint modeling. This modeling is based on wind direction and speed, as well as tower height. Plots were placed in the core footprint and their area adjusted based on footprint size and stand density to capture a representative subset of the area from which the measured carbon fluxes originated. The sampled areas included 2830 m^2 in Hainich and 2460 m^2 in Sorø. Within each plot, we collected two increment cores to the pith of all trees with a diameter at breast height (DBH, 1.3 m above the ground) >5.6 cm. Our sampling resulted in a total of 182 and 108 cores from Hainich and Sorø, respectively (Table 1). For each individual tree, we also recorded DBH (cm), height (m), crown base height (m), social status (dominant, co-dominant, or suppressed), as well as its precise location (distance and azimuth) relative to the plot center. The increment cores were dried, sanded, and polished down to a 15 μm grate, and visually dated using standard dendrochronological techniques (Schweingruber, 1996). Each tree ring was measured to the nearest 0.01 mm using a LINTAB-6 measurement system (Rinntech, Heidelberg, Germany), and the quality of the dating was checked visually and statistically using the COFECHA program (Holmes, 1983). Accurate dating of annual growth rings failed in a small number of young individuals, for which we estimated growth variability based on that of up to five randomly selected trees of the same species with a comparable DBH (±2 cm). For the long-term tree-ring chronologies at the site level for Hainich and Sorø, please refer to Fig. S2.

2.3. Tree biomass increment and BPE

To derive annual tree biomass increment, we first reconstructed historical tree DBH based on the measured DBH in the sampling year and the tree-ring width series of the respective tree. To avoid biases due to sample orientation and non-circular tree shapes, we used the proportional method put forth by Bakker (Bakker, 2005). In case an increment core did not reach the pith, we performed a pith-offset estimation based on the curvature of the last five rings using the concentric circles method (Pirie et al., 2015). Subsequently, we applied five published allometric biomass equations to calculate the aboveground biomass increment (ABI) of individual trees. Depending on the equation, ABI was estimated based on DBH alone or based on a combination of DBH and tree height to account for site-specific DBH-height relationships (Fig. S3). Given the good agreement between biomass estimates from the five equations, we used their mean in our primary analyses (Fig. S4). The individual equations are listed in Table S1, including the generalized equation from Forrester et al. (2017) that estimates the annual aboveground biomass of each tree as follows:

$$ln(Y) = ln\beta_0 + ln\,(D)\,\beta_1 + \varepsilon \quad (1)$$

where prediction of aboveground biomass (Y, kg) is calculated by the intercept ($\beta_0 = -1.6594$ for *F. sylvatica* and $\beta_0 = -2.8255$ for *F. excelsior*), slope ($\beta_1 = 2.3589$ for *F. sylvatica* and $\beta_1 = 2.8048$ for *F. excelsior*), and the independent variable tree diameter (D, cm), plus an error term ε. We then calculated the aboveground biomass increment (ABI) of each tree by subtracting its biomass in year t-1 from the biomass of in year t. To enable direct comparisons with the EC measurements [g C m^{-2} y^{-1}], we multiplied ABI by the carbon content of the wood using site-specific carbon content values (i.e., 47 % in Sorø) or estimating it at 50 % (in Hainich) (Gea-Izquierdo and Sanchez-Gonzalez, 2022; Ruiz-Peinado Gertrudix et al., 2012; Skovsgaard and Nord-Larsen, 2011). The resulting metric of aboveground carbon increment (ACI) per tree (Fig. 2) was assessed within size classes and also summed up to the plot level and expressed on a per-area basis (g C m^{-2} y^{-1}). By dividing ACI by GPP, we were then able to quantify BPE as the fraction of sequestered carbon that is allocated to aboveground structural growth each year.

2.4. Eddy covariance data

Daily sums of Net Ecosystem Exchange (NEE; gC m^{-2} d^{-1}) calculated from half-hourly EC data were derived from the FLUXNET2015 Dataset (Pastorello et al., 2020). Measurements for the remaining years towards present were obtained directly from the site principal investigators. Daily GPP estimates (gC m^{-2} d^{-1}) were aggregated from half-hourly data using the partitioning method based on daytime (Sorø) and nighttime (Hainich) respiration (i.e., GPP_NT_VUT_REF), and they were then summed up to the annual scale (Reichstein et al., 2005; Wu et al., 2013).

2.5. Climate response analysis

The relationships between climate (temperature, precipitation, and the standardized precipitation evapotranspiration index SPEI) and BPE, GPP, and ACI were analyzed using the R package dendroTools (Jevšenak and Levanič, 2018). Climate data during the flux-tower period were obtained from local meteorological observations at the study sites, whereas long-term records (1953–2017) were obtained from the gridded *E*-OBS database at a spatial resolution of 0.1°. Data were extracted for the grid cells that encompass our study sites. The SPEI was calculated

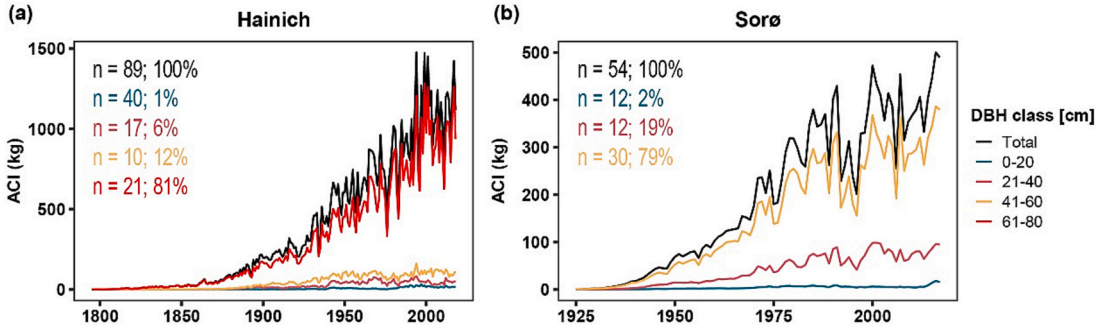

Fig. 2. Variation in annual aboveground carbon increment (ACI, kg) at the Hainich (1795–2018) and Sorø (1924–2017) sites based on the distribution of diameter at breast height (DBH, cm). DBH groups encompassed 0–20 cm, 21–40 cm, 41–60 cm, and 61–80 cm (Hainich only). n represents the number of sampled trees, and % represents the percentage of total ACI for each DBH class. When summed up to the plot level, ACI is shown in black.

using the *spei* package in R and with evapotranspiration estimated based on the Hargreaves method. Day-wise aggregated climate correlations were calculated between 1 and 270 days from June of the previous calendar year to October of the current calendar year during the shared period of 2000–2017. Within this 19-month window that encompasses most lagged and concurrent climate influences on tree growth in Europe (Babst et al., 2014), we tested all possible combinations of consecutive days (up to 270 days) to identify the most relevant climatic seasons for tree growth at our sites.

Beyond their responses to short-term climate variability, we also looked for longer-term trends in ACI, GPP, and BPE. Only the annual GPP at the Sorø site showed a significant positive trend during 1997–2017 (Fig. 3f). This data was detrended for climate response analysis by calculating the residuals of a linear model applied to the time series, which were then normalized by the percentage deviation from the mean. In order to benchmark the climate correlations obtained for the EC period, we also calculated equivalent correlations from the long-term E-OBS records of the three climate variables. Over this multi-decadal time scale, growth-climate relationships were only analyzed for detrended tree-ring width data to confirm the main limiting climate factors (Fig. S5).

2.6. Drought events detection and analysis

We expected BPE anomalies to be particularly pronounced during or after drought extremes when the differing responses of ACI and GPP should take full effect. Hence, we targeted drought episodes that occurred during the limited periods covered by the EC measurements at the two sites. We also looked for concurrent growth anomalies. Based on "Cropper values" as introduced by Cropper (1979). These values are calculated from the standard deviations of annual growth (Fig. S7), by normalizing 9-year low-pass filtered tree-ring series within a moving window centered around each year using the R packages *dplR* and *pointRes* (Bunn, 2008; Cropper, 1979; van der Maaten-Theunissen et al., 2015). Cropper values of ±1.28 (moderate growth anomaly) and ± 1.645 (extreme growth anomaly) were adopted as thresholds of pointer year classes following Jetschke et al. (2019). This way, we were able to identify growth anomalies that coincided with the occurrence of droughts during specific seasons that had emerged from our systematic climate response analyses as important for tree growth at our sites (i.e., spring and summer). To analyze the variations of BPE in response to droughts during these relevant seasons, we calculated mean temperature and total precipitation anomalies for spring (March – May) and summer (June – July) from the meteorological station data at the flux-tower sites, expressed as percent deviations from average during the EC period (Fig. S8). Specifically, seasonal droughts in 2003, 2011, and 2018 were detected at the Hainich site, while the droughts in 2006 and 2013 were observed at the Sorø site (Fig. S8). As the tree-ring record did not extend far enough towards the present to capture the growth anomaly during the 2018 drought, which was one of the most severe droughts that central Europe has experienced (Peters et al., 2020c; Salomon et al., 2022), we utilized instead the annual variation of stem

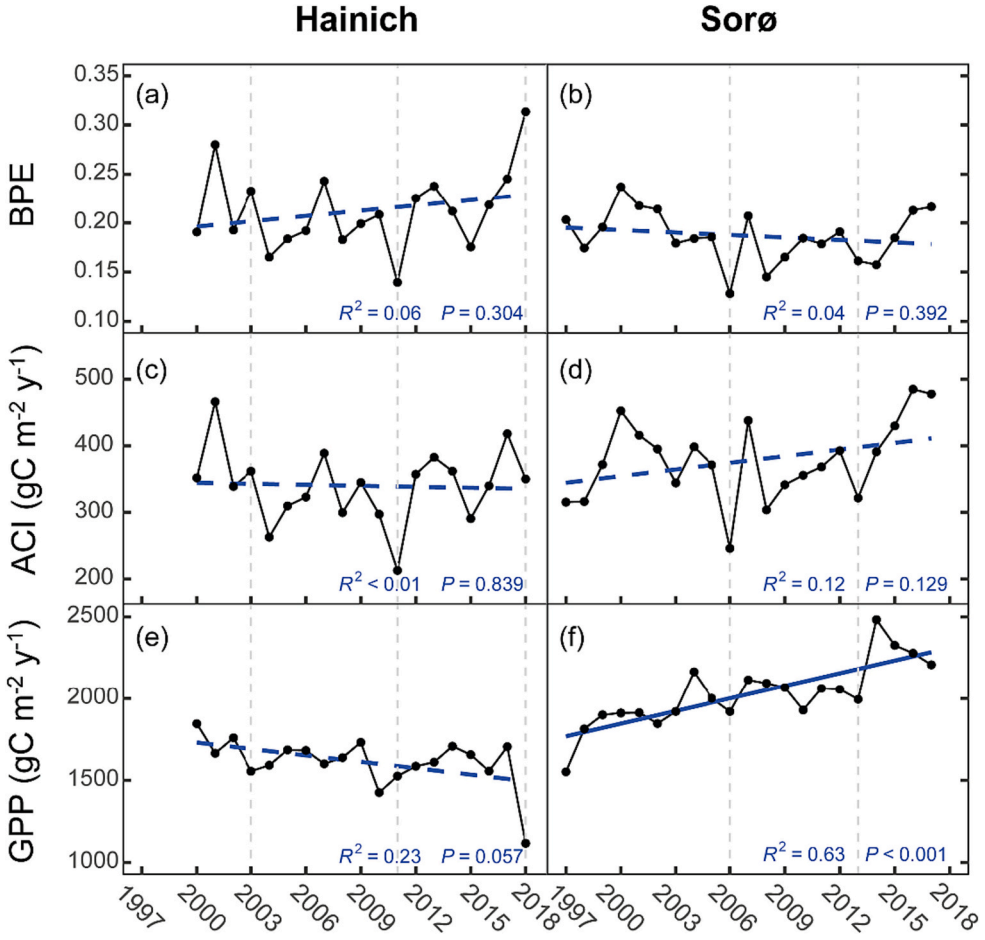

Fig. 3. Annual time series during the period of carbon flux monitoring at Hainich (2000–2018) and Sorø (1997–2017). Vertical dashed lines mark the identified drought years at Hainich (2003, 2011, and 2018) and Sorø (2006 and 2013). BPE – biomass production efficiency (=ACI/GPP); ACI – aboveground carbon increment; GPP – gross primary productivity. The dashed and solid blue lines illustrate non-significant ($p > 0.05$) and significant ($p \leq 0.05$) trends, respectively, identified through simple linear regression.

diameter measured by dendrometers at Hainich (Mund et al., 2020) to obtain the 2018 growth anomaly (see Fig. S9). All data analyses were conducted in R 4.0 (R Core Team, 2021).

3. Results

3.1. Magnitude and trends of ACI and BPE at the stand level

The primary contributors towards stand-level woody biomass stocks and increments were trees with a large diameter at breast height (DBH). As visible in Fig. 2, the magnitude and interannual variability of ACI in the largest DBH classes (61–80 cm at Hainich, 41–60 cm at Sorø) aligned closely with those of total stand-level ACI over time. These dominant DBH classes accounted for 81 % and 79 % of the total ACI for the two sites, respectively. Hence, despite comprising a relatively small subset of the total stem counts, trees with large DBH importantly control the ecosystem woody biomass and carbon sequestration, particularly in the uneven-aged forest of Hainich.

BPE showed inter-annual variability ranging between 14 and 31 % at the Hainich site and between 13 %–22 % at the Sorø site. A significant difference in BPE between these two sites was observed, as indicated by a *t*-test ($p < 0.001$). BPE trends were non-significant at both sites during the EC period (Fig. 3a and b, slope ~ 0), although a slight increase in BPE was observed at the Hainich site towards present while the annual ACI remained relatively stable at ca. 340 ± 56 g C m^{-2} y^{-1} (Fig. 3c). In contrast, Sorø exhibited a significant increasing trend in annual GPP ($R^2 = 0.63$, $p < 0.001$) that was accompanied by a less pronounced increase in annual ACI (mean = 378 ± 60 gC m^{-2} y^{-1}) during 1997–2017. Overall, the magnitude and variability of BPE were larger at Hainich compared to Sorø, indicating that, despite the lower GPP, carbon allocation to woody biomass in Hainich exceeded that of Sorø. Therefore, the parameter of interest, BPE, reveals contrasting trends and values between the two sites, reflecting the intricate relationship between GPP and ACI.

3.2. Relationship between BPE and climate variables

When focusing on drought responses, BPE exhibited a notable correlation with daily SPEI at the Sorø site (Fig. 4f), reaching two seasonal peaks in correlation coefficients (R_{max}). The first peak, with significant positive correlation coefficients ranging from 0.46 to 0.55, occurred from April 15 to May 1 (DOY 105–131) with a 25-day interval. The second peak, with significant positive correlation coefficients ranging from 0.46 to 0.59, was observed during July 23 to August 8 (DOY 204–220) with a 25-day interval. These results delineate the seasons when drought had the most negative impact on carbon allocation to woody biomass at the Sorø site. By contrast, BPE at Hainich exhibited only one period with significant positive correlations with SPEI (Fig. 4e) during the late growing season with $R_{max} = 0.55$ (DOY 232–275, 24-day interval). Together, these results indicate that Sorø was subjected to more prolonged and persistent drought effects on BPE than Hainich over the recent two decades. These results also persist through the different size classes of trees (Fig. S6), even though the drought signal in smaller trees was reduced, likely due to multiple concurrent limitations on growth.

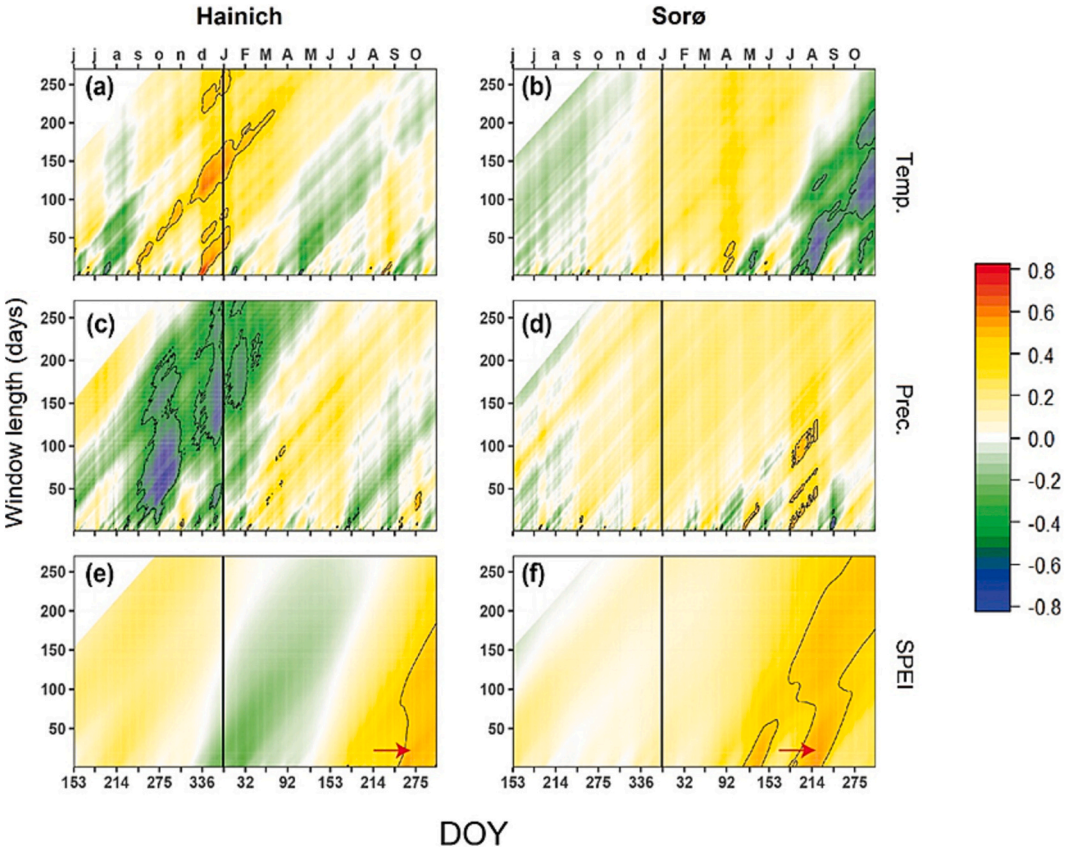

Fig. 4. Response of BPE to daily climate variables. The y-axis represents the window length of aggregated days and the x-axis represents the end of the focal window. Correlation analyses were conducted using window lengths spanning between 1 and 270 days from previous June 1st (DOY 153) to current October 31st (DOY 305) over the common period 2000–2017. Vertical lines divide the plots into the previous (left) and current years (right). Significant seasons at the $p \leq 0.05$ level are delineated by polygons. Temp. refers to daily mean air temperature (°C), Prec. refers to the daily precipitation sum (mm), SPEI is the standardized precipitation evapotranspiration index. Please see Fig. S10 for the corresponding climate response analyses for ACI and GPP and Fig. S4 for size-class specific results. Red arrows in panels e and f highlight the seasonal peaks in correlation coefficients (R_{max}) between BPE and SPEI.

In addition to SPEI, our study revealed positive correlations between BPE and spring temperature, as well as negative correlations between BPE and summer temperature at both study sites (Fig. 4a and b). In turn, correlations between BPE with summer precipitation were slightly positive (Fig. 4c and d). Overall, we found that the magnitude of the temperature signal was more noticeable than that of the precipitation signal, especially at Sorø. For example, BPE exhibited a significant positive correlation with precipitation (R_{max} = 0.59, DOY 104, 97-day interval, April 14 – July 19). Taken together, our climate response analyses support our first hypothesis (H1), evidencing that drought is a key driver of inter-annual variability in carbon allocation to woody growth at both sites.

At the seasonal level, we find that the response of BPE to June – July SPEI in Hainich is more similar to that of ACI than to that of GPP, as indicated by linear regression analysis (Fig. 5). This finding provides support for our second hypothesis (H2). Furthermore, the other observed parameters (ACI and GPP) showed different correlations with the drought index, and the strongest SPEI correlation was still found for BPE at the Sorø site for June to July (Fig. 5b, slope = 0.47). These results indicate that drought affects carbon allocation to aboveground woody biomass during the summer season. In contrast, GPP at both sites was less sensitive to summer drought than BPE or ACI (shallower slope in Fig. 5e-f) across the common period of 2001–2017.

3.3. BPE, ACI, and GPP during and after drought extremes

Droughts that occurred late in the growing season, such as the identified droughts in 2003 and 2018, had negative effects on BPE not in the concurrent, but in the following year. For example, BPE in the post-drought year 2004 at Hainich was reduced by 16.82 % compared to the mean BPE during 2000–2018 (Fig. 3a). Similarly, the annual radial growth of trees in 2019 (Fig. S9) showed reductions of 13.47 % (European beech), 5.25 % (European ash), and 27.97 % (Sycamore maple) compared to the mean during 2003–2020 for the respective species. Conversely, droughts that occurred early in the growing season such as the spring droughts in 2011 at the Hainich site, and in 2006 and 2013 at the Sorø site, exerted immediate and strong negative effects on BPE, with observed reductions of −29.36 %, −31.32 %, and − 13.81 %, respectively. In the post-drought year, a legacy effect of the spring drought 2013 for BPE was only observed in 2014 at the Sorø site, with a reduction of −15 % (Fig. 3a and b).

ACI reduction during the identified drought years was more substantial in large size classes, such as 61–80 cm at Hainich (Fig. 6a) and 41–60 cm at Sorø (Fig. 6b), indicating that trees with a bigger DBH are more sensitive to water limitation (see also Fig. S6). Similarly, the observed increase in ACI in 2003 at the Hainich site was most pronounced in the 41–60 cm and 61–80 cm DBH classes, suggesting that large trees also benefit disproportionately from abundant water resources in the early growing season. The 2003 drought occurred late in the growing season, i.e., after the tree volume increment for that year had already largely been completed, and dampened wood formation only in the following year.

GPP time series for the same detected drought and post-drought years at both sites show that droughts caused immediate GPP reductions during all drought events (Fig. 7). For instance, during the peak drought period (DOY 211–254) in the year 2003, the reduction in GPP was −32.36 % compared to the long-term average (2000–2019) at the Hainich site. In the drought year 2018, GPP was even suppressed by −57.27 % during the late summer period (DOY 174–278). Importantly, in the post-drought years, annual GPP decreased only by −0.68 %, −1.06 %, and − 11.88 % in 2004, 2012, and 2019 compared to the long-term average at Hainich, respectively. However, at the Sorø site, GPP

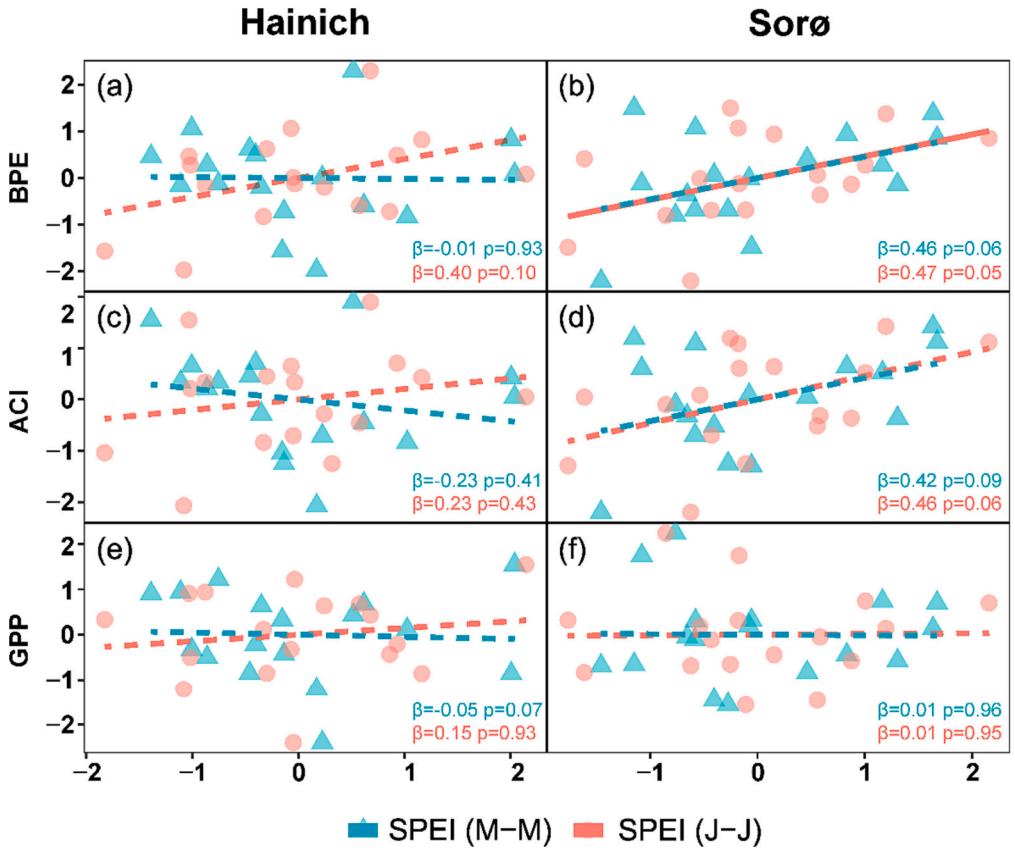

Fig. 5. Linear regression between BPE, ACI, GPP and seasonal drought at the Hainich and Sorø sites during 2001–2017. SPEI (M–M): March–May Standardized Precipitation Evapotranspiration Index; SPEI (J–J): June –July SPEI. All data were standardized by taking the residuals of a linear model and normalizing them. Slopes (β) were derived from simple linear regression. The dashed and solid lines represent non-significant and significant years, respectively.

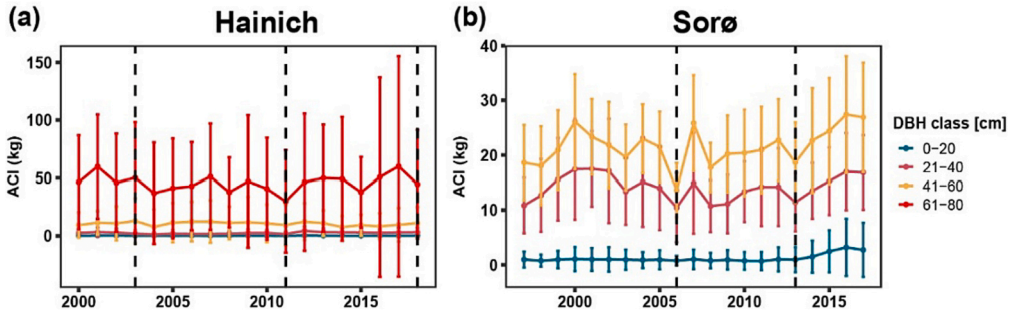

Fig. 6. Variation in ACI throughout the carbon flux period across different DBH classes at the Hainich (a) and Sorø (b) sites. DBH classes encompassed 0–20 cm, 21–40 cm, 41–60 cm, and 61–80 cm (Hainich only). Vertical dashed lines mark the identified drought years at Hainich (2003, 2011, and 2018) and Sorø (2006 and 2013). The error bars represent the standard deviation around the mean in each DBH class.

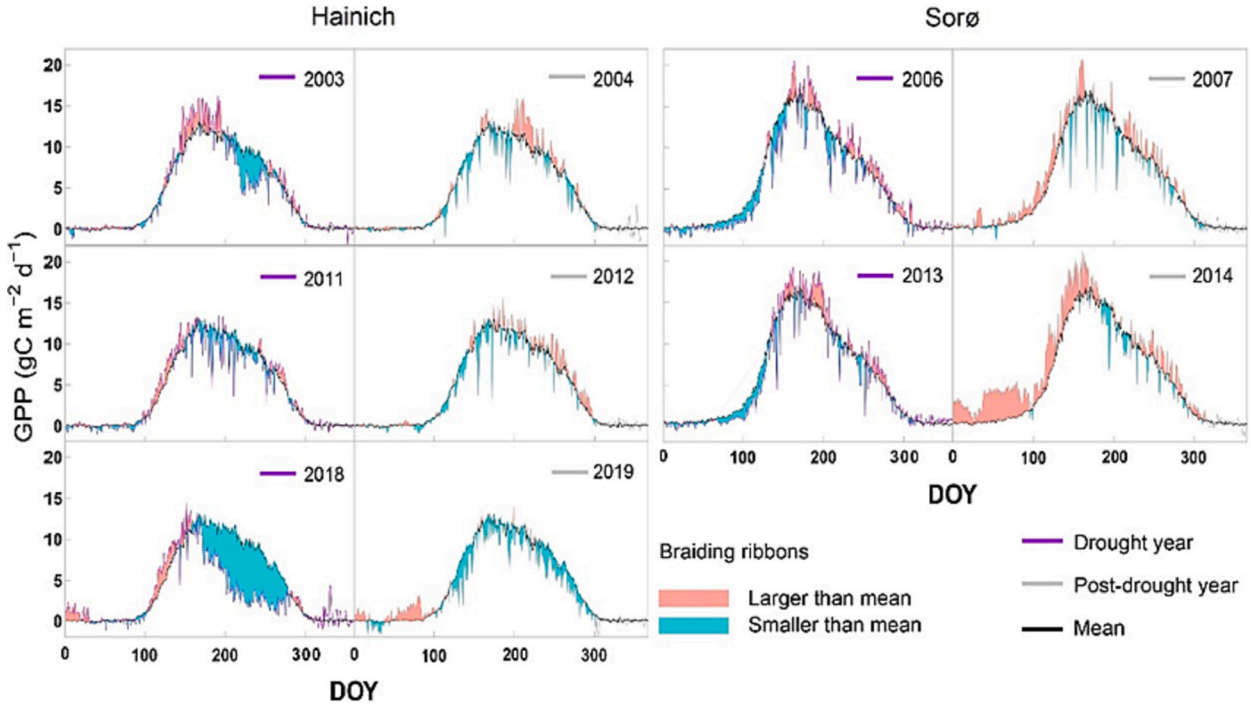

Fig. 7. Seasonal cycles of GPP anomalies during identified drought years at Hainich (2003, 2011, and 2018) and Sorø (2006 and 2013), followed by recovery in post-drought years. Areas shaded in blue represents below-average GPP for the respective days and seasons, while the red shading indicates above-average GPP compared to long-term mean fluxes for 2000–2019 at the Hainich site and 1997–2017 at the Sorø sites. DOY refers to the day of year.

increased by 4.35 % and 22.55 % in the post-drought years 2007 and 2014, respectively. Therefore, the rapid recovery of GPP compared to BPE supports our third hypothesis (H3).

4. Discussion

4.1. The interannual variation of BPE is impacted by drought

Past research on the links between GPP and tree growth has primarily focused on qualitative comparisons between the temporal variability and climate sensitivities of the two processes (e.g., Cabon et al., 2022). By focusing on the BPE parameter, our study has now explored source-sink relationships in two European beech forests in a quantitative way to assess the possible re-prioritization of carbon sinks under restrictive environmental conditions (i.e., drought). Earlier studies that have quantified BPE have covered relatively short time scales (Gea-Izquierdo and Sanchez-Gonzalez, 2022; Heid et al., 2018; Vicca et al., 2012) and could not provide a comprehensive assessment of BPE variability over annual-to-decadal scales. This has limited our understanding of how climatic factors – and drought in particular - alter the magnitude of carbon allocation to woody biomass. Our analyses of nearly 20-year time series from two European beech stands revealed a noticeable negative impact of drought on BPE during peak summer (Fig. 4). This finding is consistent with the results of Miao et al. (2022) who detected drought impacts on BPE in two coniferous plantation sites (*Pinus taeda*). There is still an active debate on the climate-driven dynamics of carbon use efficiency (CUE), which is conceptually similar to BPE but measured as the ratio of total net primary production (NPP) to GPP and supposedly remains fairly constant over time (DeLucia et al., 2007; Waring et al., 1998). This constant CUE fraction is being applied in most global carbon cycle models (Friend et al., 2019) where NPP is implemented as a direct derivative of GPP. Challenging this practice, Collalti et al. (2020) highlighted that a warming climate may enhance the efficiency of the GPP to NPP conversion, leading to increased organic matter production. Our findings support this notion of climate-driven variation in carbon allocation but instead point to a reduction of BPE under drought. Related to this, a synthesis study by Campioli et al. (2015) suggested that carbon allocation in various forest sites is not only

influenced by climate but modulated by soil fertility and management practices. We thus anticipate that future studies that include a larger number of EC sites with well-documented soil and management regimes will shed further light on BPE's response to climate variability.

4.2. The drought sensitivity of biomass growth drives changes in BPE

Our study has confirmed the initial hypothesis that the variability and climate sensitivity of BPE follow those of ACI more closely than those of GPP. This is likely a consequence of the fact that growth-related processes are highly sensitive to tree water status (Peters et al., 2020b; Fatichi et al., 2019). Interestingly, ACI reduction in response to SPEI was more pronounced in larger size classes (Fig. 6 and Fig. S6), underscoring the sensitivity of trees with bigger DBH to water limitation. Further, the largest size class in Hainich showed broad variation in ACI (Fig. 6), indicating the presence of large trees with both fast and slow growth rates. The slow-growers could be suffering from repeated drought events that caused specific individuals to reduce growth due to hydraulic damage (Arend et al., 2022). At the same time, our climate response analyses showed that drought impacts on GPP are less pronounced (Fig. S10), which is in line with earlier work showing that photosynthetically assimilated carbon is more temperature-sensitive than tree growth (Guillemot et al., 2017; Williams et al., 2014). Tree growth may thus slow down during drought, at a relatively higher rate (Hartmann et al., 2018; Korner, 2003; Muller et al., 2011). Under increased sink limitation, trees might allocate a higher proportion of their sequestered carbon towards sinks other than growth, such as non-structural carbohydrates (NSC), that may exhibit a transient increase during the initial phases of drought (Muller et al., 2011). This reprioritization is reflected by reduced BPE and a decline in the stem growth of trees (Huang et al., 2018), which can have longer-term consequences for carbon allocation dynamics at the stand level (Guillemot et al., 2017). Hence, we recommend caution when using solely carbon fluxes to estimate the magnitude and variability of the forest carbon sink.

4.3. The seasonal timing of drought plays a key role in modifying BPE

Drought impacts on tree growth increase markedly with drought duration and the seasonal timing of water limitation is equally important (Huang et al., 2018). We found that spring and summer droughts had contrasting impacts on carbon allocation: early season droughts primarily reduced current-year BPE (2011 at Hainich; 2006 and 2013 at Sorø), while late-season droughts (2003 and 2018 at Hainich) reduced the next year's BPE. The anticipated decrease in BPE in 2019 was confirmed by rapid GPP recovery (Fig. 7) and a concurrent growth decline observed in dendrometer data (Fig. S7), which we obtained to substitute the missing tree-ring data (and thus BPE) for this post-drought year. These results support existing evidence of drought legacy effects on tree growth for up to 4 years (Anderegg et al., 2015; Huang et al., 2018; Salomon et al., 2022). Also, in line with a synthesis study linking GPP and tree rings with drought legacy effects across the United States (Kannenberg et al., 2020), we found that source-limited GPP is less suppressed than sink-limited ACI after droughts. This rapid GPP recovery will further amplify the decrease of BPE as stem growth is deprioritized. Future studies will continue to unravel the complex mechanisms underlying ecosystem responses to drought by considering the various involved mechanisms in integrated studies at well-equipped ecological monitoring sites (Zweifel et al., 2023).

4.4. Uncertainty and need for future research

There are inherent scaling uncertainties in all studies that assess forest productivity based on in-situ biometric data (Babst et al., 2018). The allometric methods used for ABI quantification are mainly based on a combination of tree-rings and observed tree size in the sampling year, without corrections for historical stand dynamics of tree growth, recruitment, and mortality (Gea-Izquierdo and Sanchez-Gonzalez, 2022). This uncertainty increases rapidly back in time, decreasing the reliability of ACI data that extend more than a few decades back (Alexander et al., 2017). Yet, because the EC period at our sites covers only the past approximately 20 years, we do not expect stand dynamics to substantially affect the robustness of our ACI (and thus BPE) data.

We also note that BPE specifically quantifies the percentage of carbon that is allocated to aboveground woody biomass, whereas our study did not quantify belowground allocation to coarse and fine root biomass. This is clearly a limitation of the experimental setup at our sites as root biomass is generally assumed to equal approximately 22 % of aboveground biomass (Chojnacky et al., 2013). In individual studies targeting the Canadian boreal forest, root biomass has even accounted for 39.8 % of NPP (Smyth et al., 2013). Enabling the quantification of belowground BPE is thus an important frontier to further elucidate relative changes in carbon allocation under climatic extremes.

The management practices undertaken at Sorø have included 10 % thinning approximately every 10 years, resulting in an average annual thinning rate of 1 % (Pilegaard and Ibrom, 2020). Such practices aim at enhancing carbon allocation to stem biomass and reducing the risk of mortality by lowering competition between trees and alleviating physiological stresses (Collalti et al., 2018; Gómez-del-Campo et al., 2002). This management could thus influence the magnitude of BPE compared to a naturally grown forest. We expect, however, minimal impacts of forest management on the variability and climate sensitivity of ACI and BPE (Testolin et al., 2023). This is confirmed by our growth-climate analyses based on long-term tree-ring chronologies that demonstrate consistent drought signals for both the managed (Sorø) and near-natural (Hainich) forests between 1953 and 2017 (Fig. S5).

Drought effects on BPE observed in our study portray sink limitations on carbon accumulation in woody biomass at the inter-annual time scale. But our dataset did not allow us to trace intra-annual carbon dynamics, which could further solidify our finding that late summer drought leads to reduced carbon investment in the latewood (Cuny et al., 2015; Puchi et al., 2023). Moving forward, it will be important to assess the different seasonal patterns of BPE on time scales ranging from weeks to months to verify that growth is indeed prioritized during favorable conditions and de-prioritized when water becomes limiting (Heid et al., 2018; Merganicova et al., 2019). For example, quantitative wood anatomy can provide further insight in woody tissue formation (von Arx et al., 2016), as can X-ray computed tomography for wood biomass production and wood density (Lehnebach et al., 2021), or the regular collection of micro-cores for near-real-time measurements of xylogenesis (Rossi et al., 2006). These higher-resolved measurements can more closely link BPE to physiological processes (e.g. cell-wall thickening time) at weekly to yearly time scales, and thereby contribute to an improved understanding of the seasonal dynamics of carbon cycling within trees.

5. Conclusion

Europe has experienced a series of prolonged, dry, and hot summers since the onset of the 21st century. Assessing drought effects on the processes of carbon allocation is thus essential for predicting vegetation feedbacks to intensifying climate change. By evaluating the temporal variability in and relationship between tree-ring based ACI and carbon flux-based GPP, we quantified annual variations in BPE and constrained its response to drought at two of the longest existing EC monitoring sites in European beech stands. Our findings revealed that water stress modifies BPE by causing stronger stem growth than GPP reductions during and after drought events. We also found that the variability of BPE follows that of ACI, rather than that of GPP, indicating sink limitations on carbon allocation to woody biomass. Our findings further imply that variations in environmental constraints such as the timing of drought contribute to the decoupling of carbon uptake and allocation. Further experiments and observational networks across a broader range

of species and ecosystems will help identify the effects of drought on carbon allocation at larger scale and in species other than beech.

CRediT authorship contribution statement

Jingshu Wei: Writing – original draft, Visualization, Software, Methodology, Data curation, Conceptualization. **Georg von Arx:** Writing – review & editing, Methodology, Conceptualization. **Zexin Fan:** Writing – review & editing, Conceptualization. **Andreas Ibrom:** Writing – review & editing, Data curation. **Martina Mund:** Writing – review & editing, Data curation. **Alexander Knohl:** Writing – review & editing, Data curation. **Richard L. Peters:** Writing – review & editing, Data curation. **Flurin Babst:** Writing – review & editing, Writing – original draft, Supervision, Project administration, Methodology, Investigation, Funding acquisition, Conceptualization.

Declaration of competing interest

The authors declare that they have no conflict of interest.

Data availability

Data will be made available on request.

Acknowledgement

We acknowledge the *E*-OBS dataset from the EU-FP6 project UERRA (https://www.uerra.eu) and the Copernicus Climate Change Service, and the data providers in the ECA&D project (https://www.ecad.eu). We thank Anne Verstege and Daniel Nievergelt for their assistance with tree-ring collection, measurements, and cross-dating. We thank Jernej Jevšenak and Gu Hongshuang for their contribution to processing daily climate data. The authors also thank Yang Raoqiong for her guidance in data visualization. For the Hainich site, we acknowledge support by Niedersächsisches Vorab (DigitalForst, ZN 3679), Ministry of Lower-Saxony for Science and Culture (MWK). We thank the administration of the Hainich National Park for the opportunity for research within the National Park. We also thank Olaf Kolle, Kerstin Hippler, Karl Kübler, Martin Hertel, Agnes Fastnacht (Max-Planck Institute for Biogeochemistry), Frank Tiedemann, Dietmar Fellert, Edgar Tunsch, Anne Klosterhalfen (University of Göttingen). For the Sorø site, we acknowledge the following EU research and infrastructure projects as contributions: EUROFLUX, CARBOEUROPE, CARBOEUROPE_IP, NITROEUROPE-IP, IMECC, national ICOS-DK in support of EU ICOS, and national LTER-DK in support of EU eLTER. Flurin Babst acknowledges support from the Arizona Institute for Resilience and was also supported by the HOMING program of the Foundation for Polish Science, co-financed by the EU Regional Development Fund (POIR.04.04.00-00-5F85/18-00). Zexin Fan was supported by West Light Talent Program of the Chinese Academy of Sciences (xbzg-zdsys-202218). We appreciate the valuable feedback from 4 anonymous reviewers and from Seth Irwin for his language editing of the final version of the manuscript.

Appendix A. Supplementary data

Supplementary data to this article can be found online at https://doi.org/10.1016/j.scitotenv.2024.170726.

References

Alexander, M.R., Rollinson, C.R., Babst, F., Trouet, V., Moore, D.J.P., 2017. Relative influences of multiple sources of uncertainty on cumulative and incremental tree-ring-derived aboveground biomass estimates. Trees 32, 265–276.
Anderegg, W.R.L., Schwalm, C., Biondi, F., Camarero, J.J., Koch, G., Litvak, M., et al., 2015. Pervasive drought legacies in forest ecosystems and their implications for carbon cycle models. Science 349, 528–532.
Anderegg, W.R.L., Trugman, A.T., Wang, J., Wu, C., 2022. Open science priorities for rigorous nature-based climate solutions. PLoS Biol. 20, e3001929.
Arend, M., Link, R.M., Zahnd, C., Hoch, G., Schuldt, B., Kahmen, A., 2022. Lack of hydraulic recovery as a cause of post-drought foliage reduction and canopy decline in European beech. New Phytol. 234, 1195–1205.
Babst, F., Bouriaud, O., Papale, D., Gielen, B., Janssens, I.A., Nikinmaa, E., et al., 2014. Above-ground woody carbon sequestration measured from tree rings is coherent with net ecosystem productivity at five eddy-covariance sites. New Phytol. 201, 1289–1303.
Babst, F., Bodesheim, P., Charney, N., Friend, A.D., Girardin, M.P., Klesse, S., et al., 2018. When tree rings go global: challenges and opportunities for retro- and prospective insight. Quat. Sci. Rev. 197, 1–20.
Babst, F., Friend, A.D., Karamihalaki, M., Wei, J., von Arx, G., Papale, D., et al., 2021. Modeling ambitions outpace observations of Forest carbon allocation. Trends Plant Sci. 26, 210–219.
Bakker, J.D., 2005. A new, proportional method for reconstructing historical tree diameters. Can. J. For. Res. 35, 2515–2520.
Bosela, M., Lukac, M., Castagneri, D., Sedmak, R., Biber, P., Carrer, M., et al., 2018. Contrasting effects of environmental change on the radial growth of co-occurring beech and fir trees across Europe. Sci. Total Environ. 615, 1460–1469.
Bunn, A.G., 2008. A dendrochronology program library in R (dplR). Dendrochronologia 26, 115–124.
Cabon, A., Kannenberg, S.A., Arain, A., Babst, F., Baldocchi, D., Belmecheri, S., et al., 2022. Cross-biome synthesis of source versus sink limits to tree growth. Science 376, 758–761.
Calfapietra, C., Barbati, A., Perugini, L., Ferrari, B., Corona, P., 2015. Carbon mitigation potential of different forest ecosystems under climate change and various managements in Italy. Ecosyst. Health Sustain. 1, art25.
Campioli, M., Vicca, S., Luyssaert, S., Bilcke, J., Ceschia, E., Chapin Iii, F.S., et al., 2015. Biomass production efficiency controlled by management in temperate and boreal ecosystems. Nat. Geosci. 8, 843–846.
Carbone, M.S., Czimczik, C.I., Keenan, T.F., Murakami, P.F., Pederson, N., Schaberg, P. G., et al., 2013. Age, allocation and availability of nonstructural carbon in mature red maple trees. New Phytol. 200, 1145–1155.
Chiang, F., Mazdiyasni, O., AghaKouchak, A., 2021. Evidence of anthropogenic impacts on global drought frequency, duration, and intensity. Nat. Commun. 12, 2754.
Chojnacky, D.C., Heath, L.S., Jenkins, J.C., 2013. Updated generalized biomass equations for north American tree species. Forestry 87, 129–151.
Collalti, A., Trotta, C., Keenan, T.F., Ibrom, A., Bond-Lamberty, B., Grote, R., et al., 2018. Thinning can reduce losses in carbon use efficiency and carbon stocks in managed forests under warmer climate. J. Adv. Model Earth Syst. 10, 2427–2452.
Collalti, A., Ibrom, A., Stockmarr, A., Cescatti, A., Alkama, R., Fernandez-Martinez, M., et al., 2020. Forest production efficiency increases with growth temperature. Nat. Commun. 11, 5322.
Cropper, J.P., 1979. Tree-ring skeleton plotting by computer. In: Tree-Ring Bulletin.
Cuny, H.E., Rathgeber, C.B., Frank, D., Fonti, P., Makinen, H., Prislan, P., et al., 2015. Woody biomass production lags stem-girth increase by over one month in coniferous forests. Nat. Plants 1, 15160.
DeLucia, E.H., Drake, J.E., Thomas, R.B., Gonzalez-Meler, M., 2007. Forest carbon use efficiency: is respiration a constant fraction of gross primary production? Glob. Chang. Biol. 13, 1157–1167.
Dyderski, M.K., Paz, S., Frelich, L.E., Jagodzinski, A.M., 2018. How much does climate change threaten European forest tree species distributions? Glob. Chang. Biol. 24, 1150–1163.
Evans, M.E.K., DeRose, R.J., Klesse, S., Girardin, M.P., Heilman, K.A., Alexander, M.R., et al., 2022. Adding tree rings to North America's National Forest Inventories: an essential tool to guide drawdown of atmospheric CO2. Bioscience 72, 233–246.
Fatichi, S., Leuzinger, S., Korner, C., 2014. Moving beyond photosynthesis: from carbon source to sink-driven vegetation modeling. New Phytol. 201, 1086–1095.
Fatichi, S., Pappas, C., Zscheischler, J., Leuzinger, S., 2019. Modelling carbon sources and sinks in terrestrial vegetation. New Phytol. 221, 652–668.
Forrester, D.I., Tachauer, I.H.H., Annighoefer, P., Barbeito, I., Pretzsch, H., Ruiz-Peinado, R., et al., 2017. Generalized biomass and leaf area allometric equations for European tree species incorporating stand structure, tree age and climate. For. Ecol. Manag. 396, 160–175.
Friend, A.D., Eckes-Shephard, A.H., Fonti, P., Rademacher, T.T., Rathgeber, C.B.K., Richardson, A.D., et al., 2019. On the need to consider wood formation processes in global vegetation models and a suggested approach. Ann. For. Sci. 76.
Gea-Izquierdo, G., Sanchez-Gonzalez, M., 2022. Forest disturbances and climate constrain carbon allocation dynamics in trees. Glob. Chang. Biol. 28, 4342–4358.
Giebink, C.L., Domke, G.M., Fisher, R.A., Heilman, K.A., Moore, D.J.P., DeRose, R.J., Evans, M.E.K., 2022. The policy and ecology of forest-based climate mitigation: challenges, needs, and opportunities. Plant Soil 479, 25–52.
Gómez-del-Campo, M., Ruiz, C., Lissarrague, J.R., 2002. Effect of water stress on leaf area development, photosynthesis, and productivity in chardonnay and Airén grapevines. Am. J. Enol. Vitic. 53, 138–143.
Guillemot, J., Francois, C., Hmimina, G., Dufrene, E., Martin-StPaul, N.K., Soudani, K., et al., 2017. Environmental control of carbon allocation matters for modelling forest growth. New Phytol. 214, 180–193.
Hartmann, H., Adams, H.D., Hammond, W.M., Hoch, G., Landhäusser, S.M., Wiley, E., et al., 2018. Identifying differences in carbohydrate dynamics of seedlings and mature trees to improve carbon allocation in models for trees and forests. Environ. Exp. Bot. 152, 7–18.
He, Y., Peng, S., Liu, Y., Li, X., Wang, K., Ciais, P., Arain, M.A., Fang, Y., Fisher, J.B., Goll, D., Hayes, D., Huntzinger, D.N., Ito, A., Jain, A.K., Janssens, I.A., Mao, J., Matteo, C., Michalak, A.M., Peng, C., Peñuelas, J., Poulter, B., Qin, D., Ricciuto, D.

M., Schaefer, K., Schwalm, C.R., Shi, X., Tian, H., Vicca, S., Wei, Y., Zeng, N., Zhu, Q., 2020. Global vegetation biomass production efficiency constrained by models and observations. Glob. Chang. Biol. 26, 1474–1484.
Heid, L., Calvaruso, C., Andrianantenaina, A., Granier, A., Conil, S., Rathgeber, C.B.K., et al., 2018. Seasonal time-course of the above ground biomass production efficiency in beech trees (Fagus sylvatica L.). Ann. For. Sci. 75.
Hemes, K.S., Runkle, B.R.K., Novick, K.A., Baldocchi, D.D., Field, C.B., 2021. An ecosystem-scale flux measurement strategy to assess natural climate solutions. Environ. Sci. Technol. 55, 3494–3504.
Holmes, R.L., 1983. Computer-assisted quality control in tree-ring dating and measurement. Tree-Ring Bull. 43, 51–67.
Huang, J., Hammerbacher, A., Gershenzon, J., van Dam, N.M., Sala, A., McDowell, N.G., et al., 2021. Storage of carbon reserves in spruce trees is prioritized over growth in the face of carbon limitation. Proc. Natl. Acad. Sci. U. S. A. 118.
Huang, M., Wang, X., Keenan, T.F., Piao, S., 2018. Drought timing influences the legacy of tree growth recovery. Glob. Chang. Biol. 24, 3546–3559.
Jetschke, G., van der Maaten, E., van der Maaten-Theunissen, M., 2019. Towards the extremes: a critical analysis of pointer year detection methods. Dendrochronologia 53, 55–62.
Jevšenak, J., Levanič, T., 2018. dendroTools: R package for studying linear and nonlinear responses between tree-rings and daily environmental data. Dendrochronologia 48, 32–39.
Johnston, C., Radeloff, V.C., 2019. Global mitigation potential of carbon stored in harvested wood products. Proc. Natl. Acad. Sci. 116, 201904231.
Kannenberg, S.A., Novick, K.A., Alexander, M.R., Maxwell, J.T., Moore, D.J.P., Phillips, R.P., et al., 2019b. Linking drought legacy effects across scales: from leaves to tree rings to ecosystems. Glob. Chang. Biol. 25, 2978–2992.
Kannenberg, S.A., Schwalm, C.R., Anderegg, W.R.L., 2020. Ghosts of the past: how drought legacy effects shape forest functioning and carbon cycling. Ecol. Lett. 23, 891–901.
Kannenberg, S.A., Cabon, A., Babst, F., Belmecheri, S., Delpierre, N., Guerrieri, R., et al., 2022. Drought-induced decoupling between carbon uptake and tree growth impacts forest carbon turnover time. Agric. For. Meteorol. 322.
Klesse, S., DeRose, R.J., Guiterman, C.H., Lynch, A.M., O'Connor, C.D., Shaw, J.D., et al., 2018. Sampling bias overestimates climate change impacts on forest growth in the southwestern United States. Nat. Commun. 9, 5336.
Knohl, A., Schulze, E.-D., Kolle, O., Buchmann, N., 2003. Large carbon uptake by an unmanaged 250-year-old deciduous forest in Central Germany. Agric. For. Meteorol. 118, 151–167.
Korner, C., 2003. Carbon limitation in trees. J. Ecol. 91, 4–17.
Lehnebach, R., Campioli, M., Gričar, J., Prislan, P., Mariën, B., Beeckman, H., et al., 2021. High-resolution X-ray computed tomography: a new workflow for the analysis of Xylogenesis and intra-seasonal wood biomass production. Frontiers. Plant Sci. 12.
Luyssaert, S., Ciais, P., Piao, S.L., Schulze, E.D., Jung, M., Zaehle, S., et al., 2010. The European carbon balance. Part 3: forests. Glob. Chang. Biol. 16, 1429–1450.
Merganicova, K., Merganic, J., Lehtonen, A., Vacchiano, G., Sever, M.Z.O., Augustynczik, A.L.D., et al., 2019. Forest carbon allocation modelling under climate change. Tree Physiol. 39, 1937–1960.
Miao, G., Noormets, A., Gavazzi, M., Mitra, B., Domec, J.C., Sun, G., et al., 2022. Beyond carbon flux partitioning: carbon allocation and nonstructural carbon dynamics inferred from continuous fluxes. Ecol. Appl. 32, e2655.
Muller, B., Pantin, F., Genard, M., Turc, O., Freixes, S., Piques, M., et al., 2011. Water deficits uncouple growth from photosynthesis, increase C content, and modify the relationships between C and growth in sink organs. J. Exp. Bot. 62, 1715–1729.
Mund, M., Herbst, M., Knohl, A., Matthaus, B., Schumacher, J., Schall, P., et al., 2020. It is not just a 'trade-off': indications for sink- and source-limitation to vegetative and regenerative growth in an old-growth beech forest. New Phytol. 226, 111–125.
Nehrbass-Ahles, C., Babst, F., Klesse, S., Notzli, M., Bouriaud, O., Neukom, R., et al., 2014. The influence of sampling design on tree-ring-based quantification of forest growth. Glob. Chang. Biol. 20, 2867–2885.
Nolan, R.H., Price OF, Samson, S.A., Jenkins, M.E., Rahmani, S., Boer, M.M., 2022. Framework for assessing live fine fuel loads and biomass consumption during fire. For. Ecol. Manag. 504.
Novick, K.A., Metzger, S., Anderegg, W.R.L., Barnes, M., Cala, D.S., Guan, K., et al., 2022. Informing nature-based climate solutions for the United States with the best-available science. Glob. Chang. Biol. 28, 3778–3794.
Pappas, C., Maillet, J., Rakowski, S., Baltzer, J.L., Barr, A.G., Black, T.A., et al., 2020. Aboveground tree growth is a minor and decoupled fraction of boreal forest carbon input. Agric. For. Meteorol. 290.
Pappas, C., Babst, F., Fatichi, S., Klesse, S., Paschalis, A., Peters, R.L., 2023. A circumpolar perspective on the contribution of trees to the boreal Forest carbon balance. Boreal Forests in the Face of Climate Change 271–294.
Pastorello, G., Trotta, C., Canfora, E., Chu, H., Christianson, D., Cheah, Y.W., et al., 2020. The FLUXNET2015 dataset and the ONEFlux processing pipeline for eddy covariance data. Sci. Data 7, 225.
Peters, R.L., Arx, G., Nievergelt, D., Ibrom, A., Stillhard, J., Trotsiuk, V., et al., 2020a. Axial changes in wood functional traits have limited net effects on stem biomass increment in European beech (Fagus sylvatica). Tree Physiol. 40, 498–510.
Peters, R.L., Steppe, K., Cuny, H.E., De Pauw, D.J.W., Frank, D.C., Schaub, M., et al., 2020b. Turgor - a limiting factor for radial growth in mature conifers along an elevational gradient. New Phytol. 229, 213–229.
Peters, W., Bastos, A., Ciais, P., Vermeulen, A., 2020c. A historical, geographical and ecological perspective on the 2018 European summer drought. Philos. Trans. R. Soc. Lond. B. Biol. Sci. 375, 20190505.
Peters, R.L., Kaewmano, A., Fu, P.L., Fan, Z.X., Sterck, F., Steppe, K., et al., 2023. High vapour pressure deficit enhances turgor limitation of stem growth in an Asian tropical rainforest tree. Plant Cell Environ. 46, 2747–2762.
Pilegaard, K., Ibrom, A., 2020. Net carbon ecosystem exchange during 24 years in the Sorø beech Forest – relations to phenology and climate. Tellus Ser. B Chem. Phys. Meteorol. 72, 1–17.
Pirie, M.R., Fowler, A.M., Triggs, C.M., 2015. Assessing the accuracy of three commonly used pith offset methods applied to Agathis australis (kauri) incremental cores. Dendrochronologia 36, 60–68.
Puchi, P.F., Khomik, M., Frigo, D., Arain, M.A., Fonti, P., Gv, Arx, et al., 2023. Revealing how intra- and inter-annual variability of carbon uptake (GPP) affects wood cell biomass in an eastern white pine forest. Environ. Res. Lett. 18.
Pugh, T.A.M., Rademacher, T., Shafer, S.L., Steinkamp, J., Barichivich, J., Beckage, B., et al., 2020. Understanding the uncertainty in global forest carbon turnover. Biogeosciences 17, 3961–3989.
R Core Team, 2021. R: A Language and Environment for Statistical Computing. R Foundation for Statistical Computing, Vienna, Austria.
Reichstein, M., Falge, E., Baldocchi, D., Papale, D., Aubinet, M., Berbigier, P., et al., 2005. On the separation of net ecosystem exchange into assimilation and ecosystem respiration: review and improved algorithm. Glob. Chang. Biol. 11, 1424–1439.
Rossi, S., Anfodillo, T., Menardi, R., 2006. Trephor: a new tool for sampling microcores from tree stems. IAWA J. 27, 89–97.
Ruiz-Peinado Gertrudix, R., Montero, G., Del Rio, M., 2012. Biomass models to estimate carbon stocks for hardwood tree species. For. Syst. 21.
Sabbatini, S., Mammarella, I., Arriga, N., Fratini, G., Graf, A., 2018. Eddy covariance raw data processing for CO2 and energy fluxes calculation at ICOS ecosystem stations. Int. Agrophys. 32, 495–515.
Salomon, R.L., Peters, R.L., Zweifel, R., Sass-Klaassen, U.G.W., Stegehuis, A.I., Smiljanic, M., et al., 2022. The 2018 European heatwave led to stem dehydration but not to consistent growth reductions in forests. Nat. Commun. 13, 28.
Schweingruber, F.H., 1996. Tree Rings and Environment Dendroecology. Tree Rings & Environment Dendroecology.
Sevanto, S., Dickman, L.T., 2015. Where does the carbon go?–Plant carbon allocation under climate change. Tree Physiol. 35, 581–584.
Skovsgaard, J.P., Nord-Larsen, T., 2011. Biomass, basic density and biomass expansion factor functions for European beech (Fagus sylvatica L.) in Denmark. Eur. J. For. Res. 131, 1035–1053.
Smyth, C.E., Kurz, W.A., Neilson, E.T., Stinson, G., 2013. National-scale estimates of forest root biomass carbon stocks and associated carbon fluxes in Canada. Global Biogeochem. Cycles 27, 1262–1273.
Teets, A., Fraver, S., Weiskittel, A.R., Hollinger, D.Y., 2018. Quantifying climate–growth relationships at the stand level in a mature mixed-species conifer forest. Glob Change Biol.
Testolin, R., Dalmonech, D., Marano, G., Bagnara, M., D'Andrea, E., Matteucci, G., et al., 2023. Simulating diverse forest management options in a changing climate on a Pinus nigra subsp. laricio plantation in southern Italy. Sci. Total Environ. 857, 159361.
Thürig, E., Kaufmann, E., 2010. Increasing carbon sinks through forest management: a model-based comparison for Switzerland with its eastern plateau and eastern Alps. Eur. J. For. Res. 129, 563–572.
van der Maaten-Theunissen, M., van der Maaten, E., Bouriaud, O., 2015. pointRes: an R package to analyze pointer years and components of resilience. Dendrochronologia 35, 34–38.
van der Werf, G.W., Sass-Klaassen, U.G.W., Mohren, G.M.J., 2007. The impact of the 2003 summer drought on the intra-annual growth pattern of beech (Fagus sylvatica L.) and oak (Quercus robur L.) on a dry site in the Netherlands. Dendrochronologia 25, 103–112.
Vicca, S., Luyssaert, S., Penuelas, J., Campioli, M., Chapin 3rd, F.S., Ciais, P., et al., 2012. Fertile forests produce biomass more efficiently. Ecol. Lett. 15, 520–526.
von Arx, G., Crivellaro, A., Prendin, A.L., Cufar, K., Carrer, M., 2016. Quantitative wood anatomy-practical guidelines. Front. Plant Sci. 7, 781.
Waring, R.H., Landsberg, J.J., Williams, M., 1998. Net primary production of forests: a constant fraction of gross primary production? Tree Physiol. 18, 129–134.
Williams, I.N., Torn, M.S., Riley, W.J., Wehner, M.F., 2014. Impacts of climate extremes on gross primary production under global warming. Environ. Res. Lett. 9, 094011.
Wu, J., Larsen, K.S., van der Linden, L., Beier, C., Pilegaard, K., Ibrom, A., 2013. Synthesis on the carbon budget and cycling in a Danish, temperate deciduous forest. Agric. For. Meteorol. 181, 94–107.
Xia, J., Yuan, W., Wang, Y.P., Zhang, Q., 2017. Adaptive carbon allocation by plants enhances the terrestrial carbon sink. Sci. Rep. 7, 3341.
Yang, H., Ciais, P., Wang, Y., Huang, Y., Wigneron, J.P., Bastos, A., et al., 2021. Variations of carbon allocation and turnover time across tropical forests. Glob. Ecol. Biogeogr. 30, 1271–1285.
Zuidema, P.A., Poulter, B., Frank, D.C., 2018. A wood biology agenda to support global vegetation modelling. Trends Plant Sci. 23, 1006–1015.
Zweifel, R., Pappas, C., Peters, R.L., Babst, F., Balanzategui, D., Basler, D., et al., 2023. Networking the forest infrastructure towards near real-time monitoring - a white paper. Sci. Total Environ. 872, 162167.